

## Critical tolerance evolution: Classification of the chain-recurrent set

Carlos Argáez, Peter Giesl, Sigurdur Freyr Hafstein

*Abstract:* Complete Lyapunov functions for non-linear dynamical systems can be obtained by approximately solving a partial differential equation that describes a condition for its orbital derivative. Efficient algorithms to compute them have been implemented. The fact that the partial differential equation is not satisfied at points of the chain-recurrent set is used to determine it; more precisely, all points where the value of the orbital derivative is larger than a fixed, critical tolerance parameter, are an estimate of the chain-recurrent set. The mathematical conditions of smoothness of the orbital derivative are obtained by locally averaging the values of the orbital derivative. Furthermore, convergence to zero is avoided by normalizing the sum of the orbital derivative condition. However, the tolerance parameter to describe the chain-recurrent set has not been considered. This results in an overestimation of the chain-recurrent set. Several algorithms have been proposed to reduce the overestimation of the chain-recurrent set, but no systematic analysis on the dependence on the critical parameter has been made so far. In this paper, we focus on studying this parameter. To proceed, the chain-recurrent set is divided into different subsets of connected components; their evolution per iteration and their different behaviour are studied. The outcome of this research will create an efficient analysis method for locating the chain-recurrent set and aims to reduce its overestimation by obtaining the tightest possible tolerance parameter necessary to classify it.

### 1. Introduction

Dynamical Systems describe time-depending phenomena in terms of differential equations.

Dynamical systems have vast and diverse applications in economy, biology, physics, mathematics, etc. For an unfamiliar reader, we can point out classical dynamical systems examples such as the pendulum, the population of hunter-prey animal species, the Lorenz attractor, etc.

In general, at any given time, a dynamical system has a state in its own phase-space represented as an ordered  $n$ -tuple of numbers in the shape of vectors. In this case,  $n$  represents the problem's dimension.

The dynamics can be seen as the instructions' manual to describe the time-evolution of the system on this manifold [26, 24]. The evolution rule of the dynamical system describes all future states from a given initial one. The rule can be either deterministic, i.e. the future states depends only on the current one, or stochastic, where the rule is additionally influenced by random events.

They model real-world systems to describe their often complicated behaviour. Interesting examples can be found in, e.g. the double [13] and triple pendulum with periodic forcing [11] and dry friction [12], which leads to time-periodic and non-smooth systems, or the dynamics of the wobblestone [10].

Let us assume that we have dynamics described as a time-autonomous system of differential equations (ODE), of the form:

$$\dot{\mathbf{x}} = \mathbf{f}(\mathbf{x}), \tag{1}$$

where  $\mathbf{x} \in \mathbb{R}^n$ ,  $n \in \mathbb{N}$ .

Equation (1) represents a general, continuous-time, deterministic, autonomous dynamical system. In order to understand its dynamics, one can apply several different methods. For example, the direct solutions' calculation with many different initial conditions. However, this approach is computationally costly and can only give limited information about the general behaviour of the system.

Aleksandr Mikhailovich Lyapunov published in 1892 two methods for demonstrating stability of dynamical systems. The first one consisted in constructing a solution to the dynamical system with convergent series. The second method constructs a function  $V(x)$  around a system's attractor. The *Lyapunov function*  $V(x)$  has the advantage of corresponding to the potential function in classical dynamics. Classically, a (strict) Lyapunov function [25] is decreasing along all solution trajectories in a neighbourhood of an attractor such as an equilibrium or a periodic orbit. The function has the property of:

- (I) attaining its minimum at the attractor and
- (II) of being strictly decreasing along solutions of the ODE and therefore solutions that start close to the attractor are attracted to it.

We can illustrate this idea with a pedagogical example by considering a heavy solid ball on the top of a smooth hill. If we place the ball on top of the hill, then the ball will always remain there. However, if it is subject to an infinitesimal disturbance, then it will roll down the hill to the bottom due to the gravitational force. At the deepest point of the valley the ball will remain for all times and it would require an external force to push it up the hill. Additionally, if the ball is placed at a starting point near the equilibrium in the valley, the ball will stay near the equilibrium and, moreover, will approach the equilibrium as time tends to infinity.

In this example, the hill's top is an unstable equilibrium and its bottom is (Lyapunov) stable and an attracting equilibrium. The basin of attraction consists of all starting points, such that the ball approaches the stable equilibrium.

For this system, we could propose a Lyapunov function  $V(x)$  to be the height. According to the classical definition, the first property is fulfilled since  $x_0$  is the deepest point of the corresponding valley and the second by gravity, which forces the ball to move downhill.

Generally, when modelling (non idealized) dissipative physical systems, the free energy is an obvious candidate for a Lyapunov function. It decreases along solutions due to the system's dissipativity, hence, solutions tend to a local minimum of the energy (I).

The classical definition of a Lyapunov function can be extended to a complete Lyapunov function [17, 18, 21, 22], which characterizes the complete behaviour of the dynamical system as a consequence of its definition on the whole phase space, and not just in a neighbourhood of one particular attractor. By means of its broader information, the state-space can be divided into two disjoint areas, on which the system behaves in fundamentally different ways. The part where the flow is gradient-like, i.e. the systems flows through, and where the flow is chain-recurrent, i.e. infinitesimal perturbations can make the system recurrent.

**Definition 1.1** (Complete Lyapunov function). *A complete Lyapunov function (CLF) for the system (1) is a continuous scalar function,  $V : \mathbb{R}^n \rightarrow \mathbb{R}$  that*

- *is constant in each chain-transitive connected component of the chain-recurrent set and*
- *decreases strictly along solution trajectories in other places.*

The property of being decreasing along solutions of the ODE is expressed in the next definition.

**Definition 1.2** (Orbital Derivative). *The orbital derivative of a differential function  $V : \mathbb{R}^n \rightarrow \mathbb{R}$  along the solution to the system (1) is defined through:*

$$V'(\mathbf{x}) := \frac{d}{dt}V(\mathbf{x}) = \langle \nabla V(\mathbf{x}), \dot{\mathbf{x}} \rangle = \langle \nabla V(\mathbf{x}), \mathbf{f}(\mathbf{x}) \rangle.$$

Several methods have been proposed to compute CLFs, but they are either computationally very demanding [14, 20, 23], see also [15], or assume that the positions of the attractors are known beforehand [16].

## 2. Construction of Complete Lyapunov functions

The method to compute CLFs discussed in this paper is inspired by the construction of classical Lyapunov functions using radial basis functions (RBFs) [19]. As the authors have described the method in detail in previous publications [2, 4, 6, 5, 3, 8, 7, 9], we let a short description of the essential ideas and steps suffice.

The main idea is to use collocation using RBFs to obtain a solution to the PDE

$$V'(\mathbf{x}) = -r(\mathbf{x}), \quad r(\mathbf{x}) \geq 0. \tag{2}$$

The PDE (2) is ill-posed, unless  $r(\mathbf{x})$  is identically zero or if the chain-recurrent set of (1) is empty, both of which are not interesting. However, computing a norm-minimal function fulfilling (2) at every point  $\mathbf{x}_i \in X$ , where  $X$  is a set of collocation points, is a well-posed problem. By evaluating, where a solution to the collocation problem fails to fulfill the PDE (2), we locate the chain-recurrent set.

Several parameters have to be fixed when setting up our collocation problem, i.e. the smoothness parameters  $k, l$  of the compactly supported Wendland functions used as RBFs, the radius of their support  $c^{-1}$ , the density of the hexagonal grid used as collocation points, inversely proportional to the parameter  $\alpha_{\text{Hexa-basis}}$ , the number  $2m = |Y_{\mathbf{x}_i}|$  of evaluation points

$$Y_{\mathbf{x}_i} = \left\{ \mathbf{x}_i \pm \frac{r \cdot k \cdot \alpha_{\text{Hexa-basis}} \cdot \mathbf{f}(\mathbf{x}_i)}{m \cdot \|\mathbf{f}(\mathbf{x}_i)\|} : k \in \{1, \dots, m\} \right\}$$

per collocation point  $\mathbf{x}_i$ , aligned along the flow  $\mathbf{f}(\mathbf{x}_i)$  through the collocation point  $\mathbf{x}_i$ , and the parameter  $r \in (0, 1)$ .

Further, it has turned out to be advantageous to replace system (1) with (almost normalized)

$$\dot{\mathbf{x}} = \hat{\mathbf{f}}(\mathbf{x}), \quad \hat{\mathbf{f}}(\mathbf{x}) := \frac{\mathbf{f}(\mathbf{x})}{\sqrt{\delta^2 + \|\mathbf{f}(\mathbf{x})\|^2}}, \quad \delta^2 \text{ small (e.g. } = 10^{-8}\text{),}$$

which has the same solution trajectories and thus the same chain-recurrent set as (1), cf. [4].

Our algorithm to compute CLFs and classify the chain-recurrent set can be summarized as follows:

**Algorithm I:**

1. Create the set of collocation points  $X$  and compute the approximate solution  $v_0$  to  $V'(\mathbf{x}) = -1$  using collocation with Wendland functions, as discussed above; set  $i = 0$ .
2. For each collocation point  $\mathbf{x}_j$ , compute  $v'_i(\mathbf{y})$  for all  $\mathbf{y} \in Y_{\mathbf{x}_j}$ : if  $v'_i(\mathbf{y}) > \gamma$  for a point  $\mathbf{y} \in Y_{\mathbf{x}_j}$ , then  $\mathbf{x}_j \in X_i^0$  (chain-recurrent set), otherwise  $\mathbf{x}_j \in X_i^-$  (gradient-like flow), where  $\gamma \leq 0$  is a chosen critical value. Subindex  $i$  indicates that the approximation of the chain-recurrent set and the gradient-like flow has been obtained in the current step  $i$ .
3. Define  $\tilde{r}_j = \left( \frac{1}{2m} \sum_{\mathbf{y} \in Y_{\mathbf{x}_j}} v'_i(\mathbf{y}) \right)_-$ , where  $x_- := \max(x, 0)$ , and  $r_j = \frac{N}{\sum_{i=1}^N |\tilde{r}_i|} \tilde{r}_j$ .
4. Compute the approximate solution  $v_{i+1}$  of  $V'(\mathbf{x}_j) = r_j$  for  $j = 1, 2, \dots, N$ .
5. Set  $i \rightarrow i + 1$  and repeat steps 2 to 4.

Note that the sets  $X_i^0$  and  $X_i^-$  change in each step of the algorithm.

In the next section we perform a detailed study of the influence of the critical value  $\gamma \leq 0$  in Step 2 of the algorithm for one particular example.

### 3. Dependence of the critical value $\gamma$

To analyse the influence of the numerical values of  $\gamma$  we followed the evolution of the average orbital derivative over all points in  $X_i^0$  as a function of different critical values along 100 iterations.

Once we have obtained the orbital derivative for 100 iterations then, per iteration, we study the chain-recurrent set for 9001 different critical values. That is, for  $\gamma \in [-0.9, 0]$  with increments in steps

of  $10^{-4}$ . We then count, as a function of  $\gamma$  and the iteration, how many elements there are per periodic orbit in the approximation of the chain-recurrent as well as the average orbital derivative. For each fixed iteration, we then linearly fit using the method of least squares, the average orbital derivative as a function of  $\gamma$ . In a final analysis the slopes as a function of iteration are compared.

All our computations were done using the software *LyapXool*[1].

### 3.1. Results

#### 3.2. Two circular periodic orbits

We consider system (1) with right-hand side

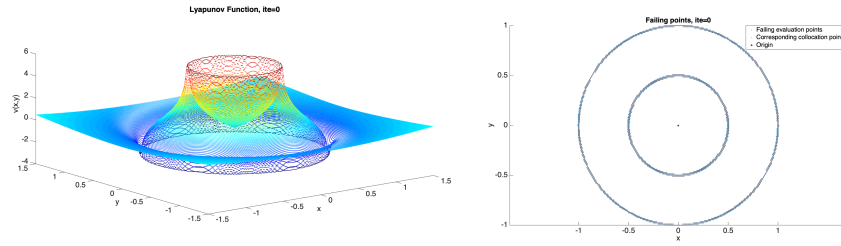
$$\mathbf{f}(x,y) = \begin{pmatrix} -x(x^2 + y^2 - 1/4)(x^2 + y^2 - 1) - y \\ -y(x^2 + y^2 - 1/4)(x^2 + y^2 - 1) + x \end{pmatrix}. \quad (3)$$

This system has two periodic circular orbits: an asymptotically stable periodic orbit at  $\Omega_1 = \{(x,y) \in \mathbb{R}^2 \mid x^2 + y^2 = 1\}$  and a repelling periodic orbit at  $\Omega_2 = \{(x,y) \in \mathbb{R}^2 \mid x^2 + y^2 = 1/4\}$ . Moreover, it has an asymptotically stable equilibrium at the origin.

To compute the CLF with our method we used the Wendland function  $\psi_{5,3}$  with  $c = 1$ . The collocation points were set in a region  $[-1.5, 1.5] \times [-1.5, 1.5] \subset \mathbb{R}^2$  and we used a hexagonal grid [19, 2, 4, 6, 5] with  $\alpha_{\text{Hexa-basis}} = 0.0129$ . The evaluation grid was computed using the directional grid with  $m = 10$ .

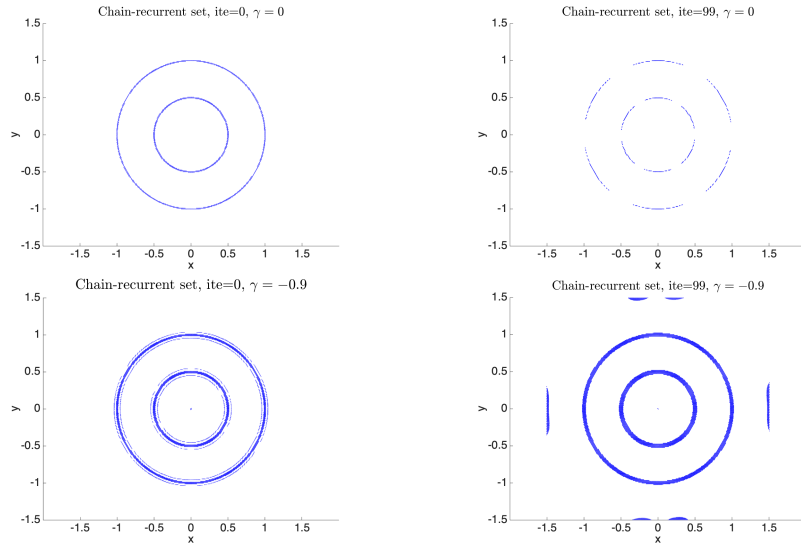
We computed this example with the almost-normalized method  $\dot{\mathbf{x}} = \hat{\mathbf{f}}(\mathbf{x})$  with  $\delta^2 = 10^{-8}$ . Finally, the limiting radius for the directional grid was set to be  $r = 0.5$ .

The CLF and its chain-recurrent set are shown in Fig. 1.



**Figure 1.** Left figure: Complete Lyapunov function at the initial iteration for system (3). Right figure: Chain-recurrent set for  $\gamma = -0.7924$ .

Let us start by showing that when approximating the chain-recurrent set, there is a strong dependence on both the number of iterations and the value of  $\gamma$ , Fig. 2.



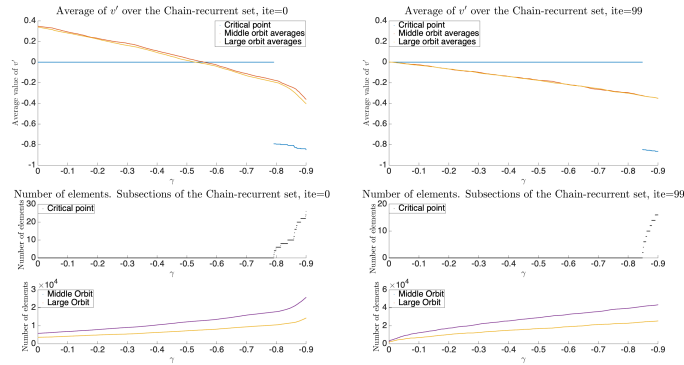
**Figure 2.** Upper left: Chain-recurrent set obtained for  $\gamma = 0$ , iteration 0. Upper right: Chain-recurrent set for  $\gamma = 0$ , iteration 99. Lower left: Chain-recurrent set obtained for  $\gamma = -0.9$ , iteration 0. Lower right: Chain-recurrent set obtained for  $\gamma = -0.9$ , iteration 99

Fig. 2 exemplifies how the description and classification of the chain-recurrent set depends not only on the value of  $\gamma$  but also in the amount of iterations. That could be seen in two different ways:

- For a fixed  $\gamma$ , different iterations give different approximations to the chain-recurrent set
- For a fixed iteration, different  $\gamma$ 's give different approximations to the chain-recurrent set

For  $\gamma = 0$ , iteration 0, we see that we do not find a critical point at the origin while we do manage to find the two closed orbits. For iteration 99, the orbits are not connected anymore. For  $\gamma = -0.9$ , we see that in both cases, iteration 0 and 99, provide overestimated chain-recurrent sets. We see, however, that the overestimation is higher for iteration 99 and there is some noise added at the boundary of the area.

In Fig. 3, we plot the average orbital derivative as well as the amount of elements in each connected component of the chain-recurrent set (i.e. the two orbits and the equilibrium) versus the critical values  $\gamma \in [-0.9, 0]$  for iterations 0 and 99.



**Figure 3.** Upper figures: average value of the orbital derivative for the connected components of the chain-recurrent set for all  $\gamma \in [-0.9, 0]$ . Left: iteration 0, right: iteration 99. Lower: amount of elements in the connected components of the chain-recurrent set for all  $\gamma \in [-0.9, 0]$ . Left: iteration 0, right: iteration 99.

First, we see in Fig. 3 that for a fixed iteration and on the orbits, the dependence of the average value of the orbital derivative is a linear function of the critical value is linear. It does not behave the same way for the critical point. The reason is that there are no elements found around the critical point for critical values higher than ca.  $-0.8$ .

We notice that as iterations grow in number, the amount of elements in the connected components increases.

Now we use the method of least squares to fit a straight line to each of the curves as in Fig. 3, for each iteration 0 to 99. We compute the slope of each of these curves and show in Fig. 4 how it changes as a functions of the iteration. Note that the slopes are constant for the two orbits after the first 10 iterations. For the equilibrium, however, the slope changes considerably more.

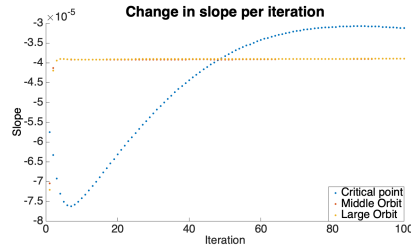


**Figure 4.** The slope of the fitted straight line, representing the function of average orbital derivative versus  $\gamma$ , as a function of iteration and for the different connected components.

The approximated chain-recurrent set  $X^0$  determined by the algorithm has too many connected components for some values. On the other hand, for other values, the periodic orbits in our example

can also break up in several parts. We now analyse for which critical values the orbits break into several parts.

The construction of the CLF in our approach, as explained in Sec. 2, is done using a collocation grid and we evaluate the orbital derivative on an evaluation grid. Since both grids are scattered, all values obtained for the CLF will be scattered too. That means that the orbits will have blank spaces between their forming points. This is shown in the lefthand side of Fig. 5. Therefore, to find the breaking points we review the approximated chain-recurrent sets looking for anomalous holes beyond the geometrical constructions properties. That is shown in the righthand side of Fig. 5.

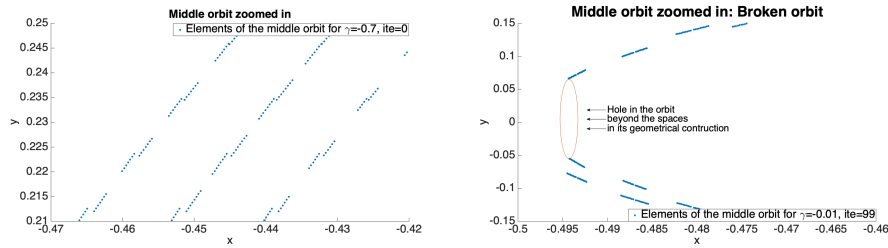


**Figure 5.** Left figure: Orbit for  $\gamma = -0.9$ . Right: Zoom in on an orbit for  $\gamma = -0.9$ .

Looking for the critical value  $\gamma_c$  for an anomalous hole to appear and break the orbit, requires considering all approximations made to the chain-recurrent set for all critical values and for all iterations.

Fig. 6 left shows  $\gamma_c$  as a function of iterations, where the value  $\gamma_c$  is such that for all  $\gamma < \gamma_c$  the orbits are connected, and for all  $\gamma \geq \gamma_c$  they are not connected. Fig. 6 right shows  $\gamma_c$  as a function of iteration, where the value  $\gamma_c$  is such that for all  $\gamma < \gamma_c$  there are no points in  $X_i^0$  near the equilibrium.

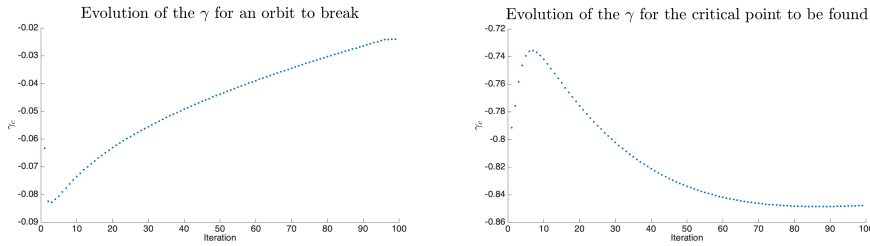


**Figure 6.** Left: Change the critical values for which the middle orbit is broken. Right: Critical value for which no equilibrium point was found. The results are shown per iteration.

### 3.3. Discussion and Conclusions

There are some remarkable observations from our study of the different numerical values for the critical parameter  $\gamma$ . First, for large negative values of  $\gamma$  the approximation  $X_i^0$  of the chain-recurrent set grows



**Table 1.** For iteration 0, amount of elements in the orbits and the critical point for  $\gamma = 0$ .

Ite	Critical Point	Middle Orbit	Large Orbit
0	0	3634	5832
99	0	1612	2524

**Table 2.** For iteration 99, amount of elements in the orbits and the critical point for  $\gamma = -0.9$ .

Ite	Critical Point	Middle Orbit	Large Orbit
0	26	14351	25822
99	16	25428	43409

as a function of iterations, for lower negative values it is the other way around. This is exemplified in tables 1 and 2. Note, however, that for  $\gamma \approx 0$  our algorithm does not identify the equilibrium at the origin as a part of the chain-recurrent set, and for  $\gamma = -0.9$  a set covering it is identified as a part of the chain-recurrent set and this set decreases in size with more iterations. It remains an open question, whether our algorithm should be used to identify the equilibrium points, that can easily be found by other and simpler means anyways, or if we should first identify them and treat their neighbourhood differently. Our results seem to indicate that our algorithm is more suited for connected components of the chain-recurrent set that are not just one point, which is not surprising because we are using a scattered grid of collocation points. Fig. 7 shows the value of the orbital derivative around the point  $(0,0)$ . The open red stars represent the values of the 99th iteration while iteration 0 is represented by the dark blue rhomboids.

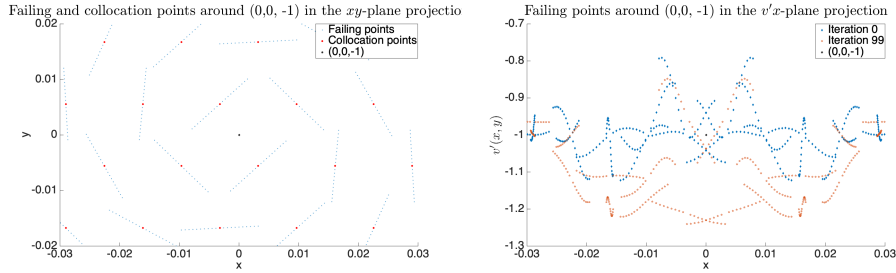


**Figure 7.** Left: Distribution of the collocation and evaluation points around the origin, as seen in the  $xy$ -plane projection. Left: Values of  $(x,y,v'(x,y))$  (graph of the orbital derivative) around the point  $(0,0,-1)$  for iterations 0 and 99, as seen in the  $xz$ -plane projection. The  $v'(x,y)$  axis the value of the orbital derivative.

Second, the evolution of the value  $\gamma_c$  of the critical value  $\gamma$  as a function of iteration is very interest-

ing. Recall that for values  $\gamma < \gamma_c$  there are gaps in the approximation  $X_i^0$  of the connected components of the chain-recurrent set. Our study shows that it is necessary to treat the approximations  $X_i^0$  as a function of  $i$  when the critical parameter  $\gamma$  is fixed. In future work we will study if it is possible to define the critical parameter  $\gamma = \gamma_i$  sensibly as a function of the iteration  $i$  such that  $X_i^0$  converges to the true chain-recurrent set. In this regard, note the effect of the normalization in Step 3 of Algorithm I. Since some collocation points are close to the chain-recurrent set, the value of the orbital-derivative at them must be close to zero. Because the sum of the absolute values of the orbital derivative at all collocation points remains fixed, it has to become more negative at other collocation points. This behaviour is not accounted for properly by having a fixed  $\gamma$ .

### Acknowledgments

The first author in this paper is supported by the Icelandic Research Fund (Rannís) grant number 163074-052, Complete Lyapunov functions: Efficient numerical computation.

### References

- [1] ARGÁEZ, C., BERTHET, J.-C., BJÖRNSSON, H., GIESL, P., AND HAFSTEIN, S. F. Lyapxool - a program to compute complete Lyapunov functions. *SoftwareX 10* (2019), 100325.
- [2] ARGÁEZ, C., GIESL, P., AND HAFSTEIN, S. *Analysing dynamical systems towards computing complete Lyapunov functions*. In Proceedings of the 7th International Conference on Simulation and Modeling Methodologies, Technologies and Applications (SIMULTECH) (2017), pp. 134–144. Madrid, Spain.
- [3] ARGÁEZ, C., GIESL, P., AND HAFSTEIN, S. *Computation of complete Lyapunov functions for three-dimensional systems*. In Proceedings IEEE Conference on Decision and Control (CDC), 2018 (2018), pp. 4059–4064. Miami Beach, FL, USA.
- [4] ARGÁEZ, C., GIESL, P., AND HAFSTEIN, S. *Computational approach for complete Lyapunov functions*. In Dynamical Systems in Theoretical Perspective. Springer Proceedings in Mathematics & Statistics. ed. Awrejcewicz J. (eds). (2018), vol. 248, pp. 1–11.
- [5] ARGÁEZ, C., GIESL, P., AND HAFSTEIN, S. *Construction of a complete Lyapunov function using quadratic programming*. In Proceedings of the 15th International Conference on Informatics in Control, Automation and Robotics (ICINCO) (2018). Porto, Portugal.
- [6] ARGÁEZ, C., GIESL, P., AND HAFSTEIN, S. *Iterative construction of complete Lyapunov functions*. In Proceedings of the 8th International Conference on Simulation and Modeling Methodologies, Technologies and Applications (SIMULTECH) (2018), pp. 211–222. Porto, Portugal.
- [7] ARGÁEZ, C., GIESL, P., AND HAFSTEIN, S. *Clustering algorithm for generalized recurrences using complete Lyapunov functions*. In Proceedings of the 16th International Conference on Informatics in Control, Automation and Robotics (ICINCO) (2019), pp. 138–146. Prague 2019, Czech Republic.

- [8] ARGÁEZ, C., GIESL, P., AND HAFSTEIN, S. *Improved estimation of the chain-recurrent set.* In Proceedings of the 18th European Control Conference (ECC) (2019), pp. 1622–1627. Naples, Italy.
- [9] ARGÁEZ, C., GIESL, P., AND HAFSTEIN, S. *Iterative construction of complete lyapunov functions: Analysis of algorithm efficiency.* To be published.
- [10] AWREJCEWICZA, J., AND KUDRA, G. *Mathematical modelling and simulation of the bifurcational wobblestone dynamics.* Discontinuity, Nonlinearity, and Complexity 3 (2014), 123–132.
- [11] AWREJCEWICZA, J., KUDRA, G., AND WASILEWSKI, G. *Experimental and numerical investigation of chaotic regions in the triple physical pendulum.* Nonlinear Dyn 50 (2007), 755–766.
- [12] AWREJCEWICZA, J., KUDRA, G., AND WASILEWSKI, G. *Chaotic zones in triple pendulum dynamics observed experimentally and numerically.* App. Mech. and Mat. 9 (2008), 1–17.
- [13] AWREJCEWICZA, J., WASILEWSKIA, G., KUDRA, G., AND RESHMINB, S. *An experiment with swinging up a double pendulum using feedback control.* JCSS 51 (2014), 176–182.
- [14] BAN, H., AND KALIES, W. *A computational approach to conley’s decomposition theorem.* J Comput Nonlin Dyn 1 (2006), 312–319.
- [15] BJÖRNSSON, J., GIESL, P., AND HAFSTEIN, S. *Algorithmic verification of approximations to complete Lyapunov functions.* Proceedings of the 21st International Symposium on Mathematical Theory of Networks and Systems 180 (2014), 1181–1188. (MTNS), Groningen, The Netherlands.
- [16] BJÖRNSSON, J., GIESL, P., HAFSTEIN, S., KELLETT, C., AND LI, H. *Computation of lyapunov functions for systems with multiple attractors.* Discrete Contin. Dyn. Syst. 9 (2015), 4019–4039.
- [17] CONLEY, C. *Isolated Invariant Sets and the Morse Index.* CBMS Regional Conference Series no. 38. American Mathematical Society, 1978.
- [18] CONLEY, C. *The gradient structure of a flow I.* Ergodic Theory Dynam. Systems 8 (1988), 11–26.
- [19] GIESL, P. *Construction of Global Lyapunov Functions Using Radial Basis Functions.* Lecture Notes in Math. 1904, Springer, 2007.
- [20] GOULLET, A., HARKER, S., MISCHAIKOW, K., KALIES, W., AND KASTI, D. *Efficient computation of Lyapunov functions for Morse decompositions.* Discrete Contin. Dyn. Syst. Ser. B 20 (2015), 2419–2451.
- [21] HURLEY, M. *Chain recurrence, semiflows, and gradients.* J Dyn Diff Equat 7, 3 (1995), 437–456.
- [22] HURLEY, M. *Lyapunov functions and attractors in arbitrary metric spaces.* Proc. Amer. Math. Soc. 126 (1998), 245–256.
- [23] KALIES, W., MISCHAIKOW, K., AND VANDERVORST, R. *An algorithmic approach to chain recurrence.* Foundations of Computational Mathematics 5 (2005), 409–449.

- [24] KATOK, A.; HASSELBLATT, B. *Introduction to the Modern Theory of Dynamical Systems*. Cambridge: Cambridge University Press, 1995.
- [25] LYAPUNOV, A. M. *The general problem of the stability of motion*. Internat. J. Control 55, 3 (1992), 521–790. Translated by A. T. Fuller from Édouard Davaux's French translation (1907) of the 1892 Russian original.
- [26] STROGATZ, S. H. *Nonlinear Dynamics and Chaos: with Applications to Physics, Biology and Chemistry*. Perseus, 2001.

Carlos Argáez, Ph.D.: Science Institute, University of Iceland, Dunhagi 5, 107 Reykjavík, Iceland ([carlos@hi.is](mailto:carlos@hi.is)).

Peter Giesl, Ph.D.: Department of Mathematics, University of Sussex, Falmer, BN1 9QH, UK ([P.A.Giesl@sussex.ac.uk](mailto:P.A.Giesl@sussex.ac.uk)).

Sigurdur Hafstein, Ph.D.: Science Institute, University of Iceland, Dunhagi 5, 107 Reykjavík, Iceland ([shafstein@hi.is](mailto:shafstein@hi.is)).